

Interaction of *OIP5-AS1* with *MEF2C* mRNA promotes myogenic gene expression

Jen-Hao Yang, Ming-Wen Chang, Poonam R. Pandey, Dimitrios Tsitsipatis, Xiaoling Yang, Jennifer L. Martindale, Rachel Munk, Supriyo De, Kotb Abdelmohsen and Myriam Gorospe *

Laboratory of Genetics and Genomics, National Institute on Aging Intramural Research Program, National Institutes of Health, Baltimore, MD 21224, USA

Received February 07, 2020; Revised November 06, 2020; Editorial Decision November 09, 2020; Accepted November 10, 2020

ABSTRACT

Long noncoding (lnc)RNAs potently regulate gene expression programs in physiology and disease. Here, we describe a key function for lncRNA *OIP5-AS1* in myogenesis, the process whereby myoblasts differentiate into myotubes during muscle development and muscle regeneration after injury. In human myoblasts, *OIP5-AS1* levels increased robustly early in myogenesis, and its loss attenuated myogenic differentiation and potently reduced the levels of the myogenic transcription factor *MEF2C*. This effect relied upon the partial complementarity of *OIP5-AS1* with *MEF2C* mRNA and the presence of HuR, an RNA-binding protein (RBP) with affinity for both transcripts. Remarkably, HuR binding to *MEF2C* mRNA, which stabilized *MEF2C* mRNA and increased *MEF2C* abundance, was lost after *OIP5-AS1* silencing, suggesting that *OIP5-AS1* might serve as a scaffold to enhance HuR binding to *MEF2C* mRNA, in turn increasing *MEF2C* production. These results highlight a mechanism whereby a lncRNA promotes myogenesis by enhancing the interaction of an RBP and a myogenic mRNA.

INTRODUCTION

In the human genome, merely 2% of expressed transcripts are protein-coding RNAs, while the rest are noncoding (nc)RNAs. Among ncRNAs, the largest portion is comprised of long noncoding (lnc)RNAs, defined as being >200 nucleotides in length. LncRNAs potently regulate gene expression program at different levels, including chromatin remodeling, RNA transcription, mRNA transport, stability, and translation, as well as protein half-life, localization and function (1–3). In contrast to protein-coding RNAs (mRNAs), some lncRNAs show highly specific tissue distribution, suggesting that they may have regulatory roles re-

stricted to certain tissues. In this regard, a growing number of studies have implicated lncRNAs in specific developmental and disease processes such as tumorigenesis, adipogenesis, neurogenesis, and myogenesis (1,2).

Myogenesis is a tightly regulated process that occurs during embryonic development and in adult skeletal muscle responding to injury (4). It begins when satellite cells are activated into myoblasts, which subsequently transform and fuse into long multinucleated myotubes, the contractile structures that enable skeletal muscle function. With advancing age, the progressive inability to maintain muscle homeostasis leads to sarcopenia and cachexia (5,6).

Protein regulators of myogenesis include a number of transcription factors, such as MYOD (myoblast determination protein D) and MYF5, which govern the initial steps in skeletal myoblast differentiation, and by myogenin (MYOG), myogenic regulatory factor (MRF)4, and myocyte-specific enhancer factors (MEF2A and MEF2C), which mediate later differentiation stages in myogenesis (7). A number of RNA-binding proteins have also been identified as key regulators of myogenic programs, including AUF1 (AU-binding factor 1), CUGBP1 (CUG triplet repeat RNA-binding protein 1), LIN28, KHSRP (K-homology splicing regulatory protein), and human antigen R (HuR) (4,8). HuR promotes myogenesis by binding the mRNAs encoding myogenic proteins such as MYOD and MYOG (9,10).

Besides regulatory proteins, a number of regulatory lncRNAs have been implicated in myogenesis (11). For example, *lincMD1* acts as a competing endogenous RNA (ceRNA) that controls myogenesis by sponging the microRNAs miR-135 and miR-133a (12), *lncMyoD* regulates myoblast differentiation by suppressing translation of IMP2 (13), and *lnc-mg* promotes myogenesis and prevents muscle atrophy by sequestering miR-125b (14). However, the functions of most muscle lncRNAs remain unexplored.

In a recent survey to identify lncRNAs differentially expressed in human myoblasts differentiating to myotubes, we found that the abundant and conserved lncRNA *OIP5-AS1*

*To whom correspondence should be addressed. Tel: +1 410 454 8412; Email: gorospem@grc.nia.nih.gov

(15), was upregulated during myogenesis [GSE136004 and GSE92632]. *OIP5-AS1* was previously implicated in biological functions including neuronal activity, stem cell maintenance, and cancer cell proliferation (15–18). Although *OIP5-AS1* is most abundant in the brain (18), it is also highly expressed in skeletal muscle. In cancer cells, the association of *OIP5-AS1* with HuR was found to prevent HuR binding to mRNAs encoding cyclin D1 (CCND1) and SIRT1, and to reduce cell proliferation (16). Here, we report that *OIP5-AS1* increased early in myogenesis and that silencing *OIP5-AS1* potently attenuated myogenic differentiation, suggesting that *OIP5-AS1* promoted myogenesis. The mechanism responsible for this regulation was linked to the interaction of *OIP5-AS1* with the 3'UTR of *MEF2C* mRNA. While HuR interacted with both transcripts in myoblasts, HuR bound to *MEF2C* mRNA optimally only in the presence of *OIP5-AS1*. In turn, HuR binding to *MEF2C* mRNA led to stabilization of *MEF2C* mRNA, raising MEF2C levels and enhancing myogenesis. Collectively, we propose that *OIP5-AS1* serves as a scaffold to recruit HuR to *MEF2C* mRNA, inducing MEF2C production and promoting skeletal muscle differentiation.

MATERIALS AND METHODS

Cell culture, myogenic differentiation, and creatine kinase activity

Mouse C2C12 myoblasts cells were cultured in growth medium (Dulbecco's modified Eagle's medium (DMEM), Life Technologies) supplemented with 20% fetal bovine serum (FBS, Gibco) and antibiotics (Life Technologies). Immortalized human AB1167 and AB678 myoblasts, developed as described (19), were cultured in growth medium (equal volume mixture of Hamm's F10 media with 20% FBS and Promocell Skeletal Muscle Cell Growth Medium). Mouse C2C12 and human AB1167 as well as human AB678 cells were induced to differentiate by growth to high density and replacement of the growth medium with differentiation medium (DMEM with 2% horse serum). Human kidney embryonic HEK293 fibroblasts were cultured in DMEM with 10% FBS and antibiotics. For silencing experiments, using a final concentration of 50 nM siRNA and Lipofectamine 2000 (Life Technologies), control small interfering RNA (Ctrl siRNA), *OIP5-AS1* siRNA or HuR siRNA was transfected 24 h before induction of differentiation. Creatine kinase (CK) activity was determined in cell lysates by using the EnzyChrom creatine kinase assay kit (BioAssay Systems) following the manufacturer's protocol. Briefly, cell lysates (1 or 2 μ g) were incubated with 10 μ l substrate solution, 100 μ l assay buffer and 1 μ l enzyme mix at 37°C for 20 min; reactions were read 20 and 40 min later at 340 nm. CK activity was calculated by the equation $CK = (OD_{40min} - OD_{20min}) / (OD_{CALIBRATOR} - OD_{H_2O}) \times 150$, and expressed as 'units per μ g of total protein' or 'fold change'.

Reverse transcription (RT) followed by real-time quantitative (q)PCR analysis

Total RNA from cultured cells was isolated using the Direct-zol™ RNA MiniPrep kit (Zymo Research), which in-

cludes a digestion step using DNase I. Total RNA from ribonucleoprotein immunoprecipitation (RIP, below) and pulldown assays was isolated using TRIzol (Life Technologies) following the manufacturer's protocol, and subsequently digested with DNase I. For cDNA synthesis, reverse transcription (RT) was performed for RNA prepared in TRIzol using Maxima reverse transcriptase following the manufacturer's protocol (Thermo Fisher Scientific). qPCR analysis of RNA was performed according to the manufacturer's instructions for KAPA SYBR FAST ABI Prism qPCR kit (KAPA Biosystems) with specific primers (Supplementary Table S1). RT-qPCR reactions were performed on QuantStudio 5 Real-Time PCR System (Thermo Fisher Scientific) with a cycle setup of 2 min at 95°C and 40 cycles of 5 s at 95°C plus 20 s at 60°C; the fold change in abundance was calculated as described previously (20,21). In qPCR amplification reactions, control 'RT minus' ('RT⁻') reactions were routinely included.

Pulldown of endogenous lncRNA by biotinylated antisense oligo (ASO)

For affinity pulldown of endogenous human *OIP5-AS1*, human myoblast lysates were prepared using PEB (20 mM Tris-HCl [pH 7.5], 100 mM KCl, 5 mM MgCl₂ and 0.5% NP-40) containing protease inhibitors (Roche) and RNase inhibitor (Thermo Fisher). The lysates were incubated with 100 pmol of biotin-labeled DNA oligomers complementary to *OIP5-AS1* for 2 h at 4°C as described previously (21). The biotinylated ASO is shown in Supplementary Table S2. RNA complexes were washed with NT2 buffer (50 mM Tris-HCl at pH 7.5, 150 mM NaCl, 1 mM MgCl₂ and 0.05% NP-40) and isolated with Dynabeads M-280 Streptavidin beads (Invitrogen).

Western blot analysis and immunofluorescence

Total protein lysates were prepared in RIPA buffer containing protease inhibitors. Proteins were size-separated by SDS-PAGE and transferred onto nitrocellulose membrane (Life Technologies). For western blot analysis, primary antibodies recognizing HuR (3A2, #L1616), MYOG (F5D, #A6020), MYH (MHC; B-5, #B0620) or HSP90 (F-8, #C2017) were from Santa Cruz Biotechnology, and those recognizing MYOD1 (D8G3, Lot 2) or MEF2C (D80C1, Lot 1) were from Cell Signaling. After incubation with the appropriate secondary antibodies, protein signals were developed using chemiluminescence. Antibody B-5, #B0620 (Santa Cruz Biotechnology) was used to detect MYH by immunofluorescence; staining with DAPI (4',6-diamidino-2-phenylindole) was used to identify nuclei.

Cloning and luciferase assay

Briefly, 3'UTR fragments of *MEF2C* mRNA were amplified with specific primers and the resulting products inserted into the psiCHECK2 plasmid downstream of the Renilla open reading frame (ORF). For reporter assays, psiCHECK2-*MEF2C*-3'UTR fragment plasmids were transfected using Lipofectamine 2000 (Invitrogen); 24 h

later, cells were induced to differentiate for 16 h and lysed. The reporter Renilla luciferase (RL) and firefly luciferase (FL) activities were analyzed using a dual-luciferase assay kit (Promega) following the manufacturer's protocol.

RIP assay

As described earlier (21), for immunoprecipitation of endogenous RNP complexes (RIP analysis) cells were lysed with PEB buffer for 10 min on ice and centrifuged at $10\,000 \times g$ for 15 min at 4°C . The supernatants were incubated with protein A Sepharose beads (GE Healthcare) coated with antibodies that recognized HuR or control IgG (Santa Cruz Biotechnology) for 3 h at 4°C . The beads were washed with NT2 buffer (50 mM Tris-HCl [pH 7.5], 150 mM NaCl, 1 mM MgCl_2 , 0.05% NP-40). The RNP complexes were incubated with 20 units of DNase I (15 min at 37°C) and further incubated with 0.1% SDS/0.5 mg/ml Proteinase K (15 min at 55°C) to remove DNA and proteins, respectively. The RNA isolated from the IP materials was further assessed by RT-qPCR analysis.

Statistical analysis

The results are represented as the means \pm SEM. Statistical comparisons of the results were evaluated using unpaired, two-tailed Student's *t*-test. A *P*-value of <0.05 was considered statistically significant and indicated in the Figures as * $P < 0.05$, ** $P < 0.01$ and *** $P < 0.001$.

RESULTS

OIP5-AS1 increases in human myoblasts differentiating into myotubes

Mouse C2C12 myoblasts are the most widely used cell culture system for the study of skeletal myogenesis. However, lncRNAs are poorly conserved between human and mouse (22). To investigate human lncRNAs in myogenesis, we examined human myoblast cell lines AB1167, AB678 and KM155 (19), cultured them to high density, and switched the cultures to media containing 2% horse serum for up to an additional 5 days. We first examined morphology changes, myogenic gene expression patterns, and myogenic enzyme activity. Similar to mouse C2C12 myoblasts (23,24), human AB1167 myoblasts differentiated progressively to form multinucleated myotubes, although at a faster pace and reaching larger myotube diameters (Figure 1A; Supplementary Figure S1). AB1167 myogenesis was accompanied by the expression of myogenic markers *MYOD*, *MYOG*, *MYH* (myosin heavy chain, MHC) and *MEF2C* mRNAs (Figure 1B), as determined by reverse transcription (RT) followed by real-time, quantitative (q)PCR analysis, and also by a time-dependent rise in proteins MYOD, MYOG, MEF2C and MYH, as determined by western blot analysis (Figure 1C). The activity of the myogenic marker enzyme creatine kinase also increased as myogenesis progressed (Figure 1D). We characterized other human myoblast lines, including AB678 (Supplementary Figure S2) and KM155 (not shown), observing similar results. During recent studies of myogenic noncoding RNAs, we found that

the levels of the abundant lncRNA *Oip5-as1* increased during C2C12 myogenesis (not shown). Here, RT-qPCR analysis revealed a rise in the levels of human *OIP5-AS1* during the early stages of human myogenesis and sustained high expression of *OIP5-AS1* afterwards (Figure 1E, Supplementary Figure S2D). In sum, along with changes in classic differentiation markers, the levels of lncRNA *OIP5-AS1* increase progressively and remain elevated in human myogenesis.

Silencing *OIP5-AS1* attenuates myogenesis in human myoblasts

To investigate a possible role for *OIP5-AS1* in myogenesis, we silenced *OIP5-AS1* in human AB1167 myoblasts using two different siRNAs (Figure 2A and Supplementary Figure S3A). Using siRNA #1, we found that silencing *OIP5-AS1* suppressed myogenesis, as determined by monitoring myotube formation, including reductions in the size and number of myotubes, as well as the number of nuclei per myotube after differentiating for 2 and 3 days (Figure 2B); similar results were observed using *OIP5-AS1* siRNA #2 (Supplementary Figure S3B). Quantification of the myotubes formed revealed that silencing *OIP5-AS1* reduced the fusion index from $\sim 80\%$ to 40% after 2 days of differentiation, and that the average of number of nuclei per myotube declined from 14 to 4 (Figure 2C). Beyond 3 days, control cultures displayed fusion of very large myotubes with few discrete edges, while distinct myotubes were still visible in the culture with silenced *OIP5-AS1* (Figure 2B).

Further evidence that myogenesis was suppressed after silencing of *OIP5-AS1* was found at 16 and 24 h of differentiation, when there was a marked decline in the levels of *MYOG* mRNA, encoding the early myogenic transcription factor MYOG, as measured by RT-qPCR analysis (Figure 2D); as *MYOD* mRNA and MYOD protein expression levels peaked before *OIP5-AS1* did, these markers were not significantly affected by *OIP5-AS1* silencing (not shown). However, silencing *OIP5-AS1* strongly delayed the production of the late differentiation marker *MYH* mRNA between 24 and 72 h, as assessed by RT-qPCR analysis (Figure 2D). In keeping with the fact that MYOG protein is an early differentiation marker and MYH protein is a late differentiation marker (Figure 1B, C), western blot analysis revealed that the levels of MYOG were lower in the *OIP5-AS1*-silenced culture starting from 24 h of differentiation, while MYH levels were decreased starting at 36 h of differentiation. In sum, *MYOG* mRNA and MYOG protein, as well as *MYH* mRNA and MYH protein showed a delayed pattern of expression in differentiating myoblasts after silencing *OIP5-AS1* compared with control cells (Figure 2D, E). Myogenic differentiation was also monitored by measuring creatine kinase activity. Compared with control myoblasts, silencing *OIP5-AS1* reduced creatine kinase activity as determined at 24, 36, 48 and 72 h (Figure 2F). These parameters were measured in other human myoblast cell lines with similar results (Supplementary Figure S3C–F). Taken together, these results support the notion that *OIP5-AS1* is required for the timely progression of skeletal myogenesis.

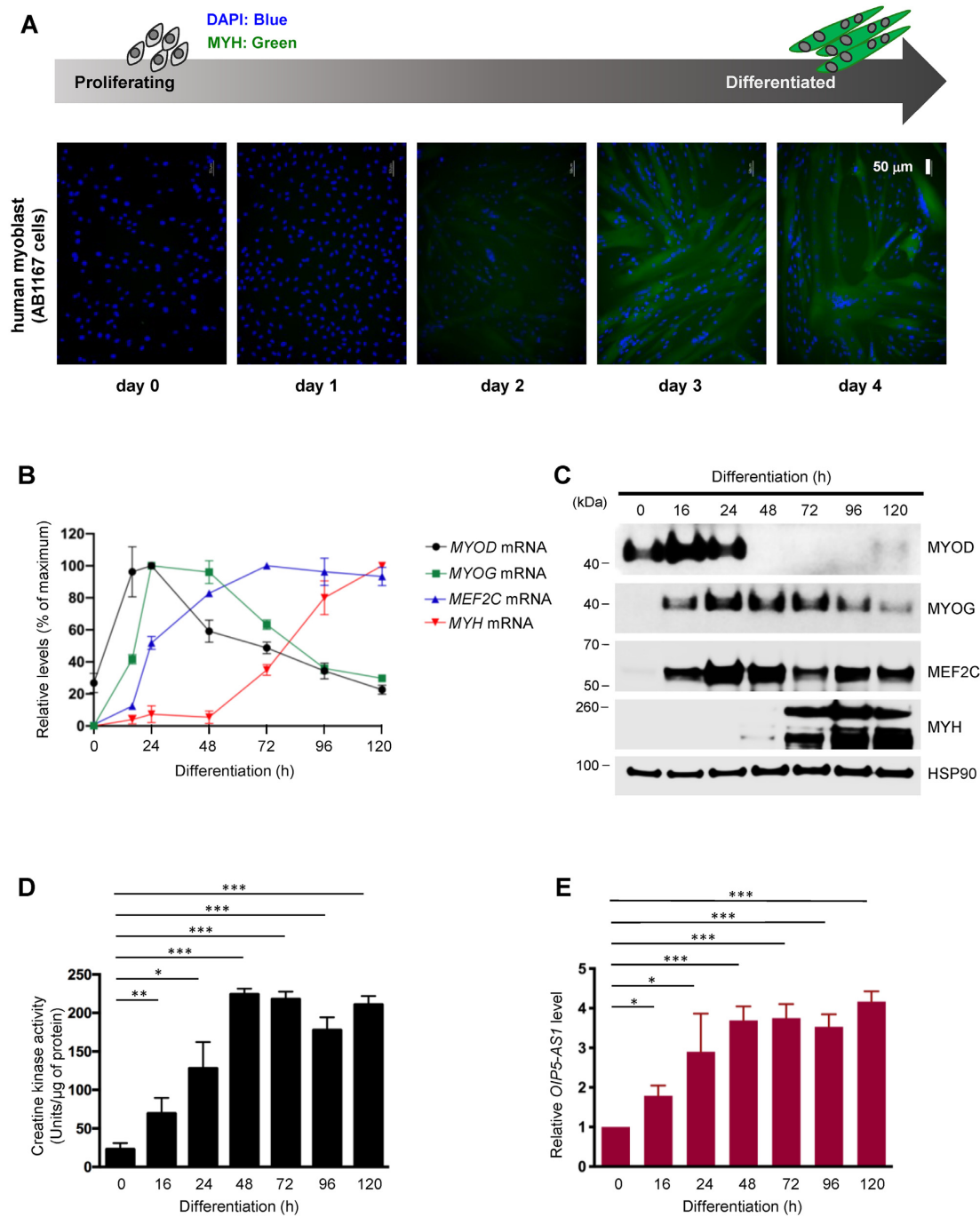


Figure 1. *OIP5-AS1* is upregulated early during myogenesis. (A) Fluorescent micrographs detecting MYH to monitor the progression of human (AB1167) myoblasts (day 0, when MYH is undetectable) to myotubes (day 4, which express high levels of MYH). Staining with DAPI was used to identify nuclei. (B–E) At the times indicated in differentiating AB1167 cultures, the relative levels of myogenic mRNAs were detected by RT-qPCR analysis and plotted as a percent of the maximum levels observed during myogenesis (B), the levels of myogenic proteins were assessed by western blot analysis (C), the levels of creatine kinase activity were measured enzymatically (Materials and Methods) (D), and the levels of *OIP5-AS1* were quantified by RT-qPCR analysis (E). Data in (B, D, E) are the means \pm SEM from three or more biological replicates. Significance was established using Student's *t*-test. **P* < 0.05; ***P* < 0.01; ****P* < 0.001. Other data are representative of three or more biological replicates.

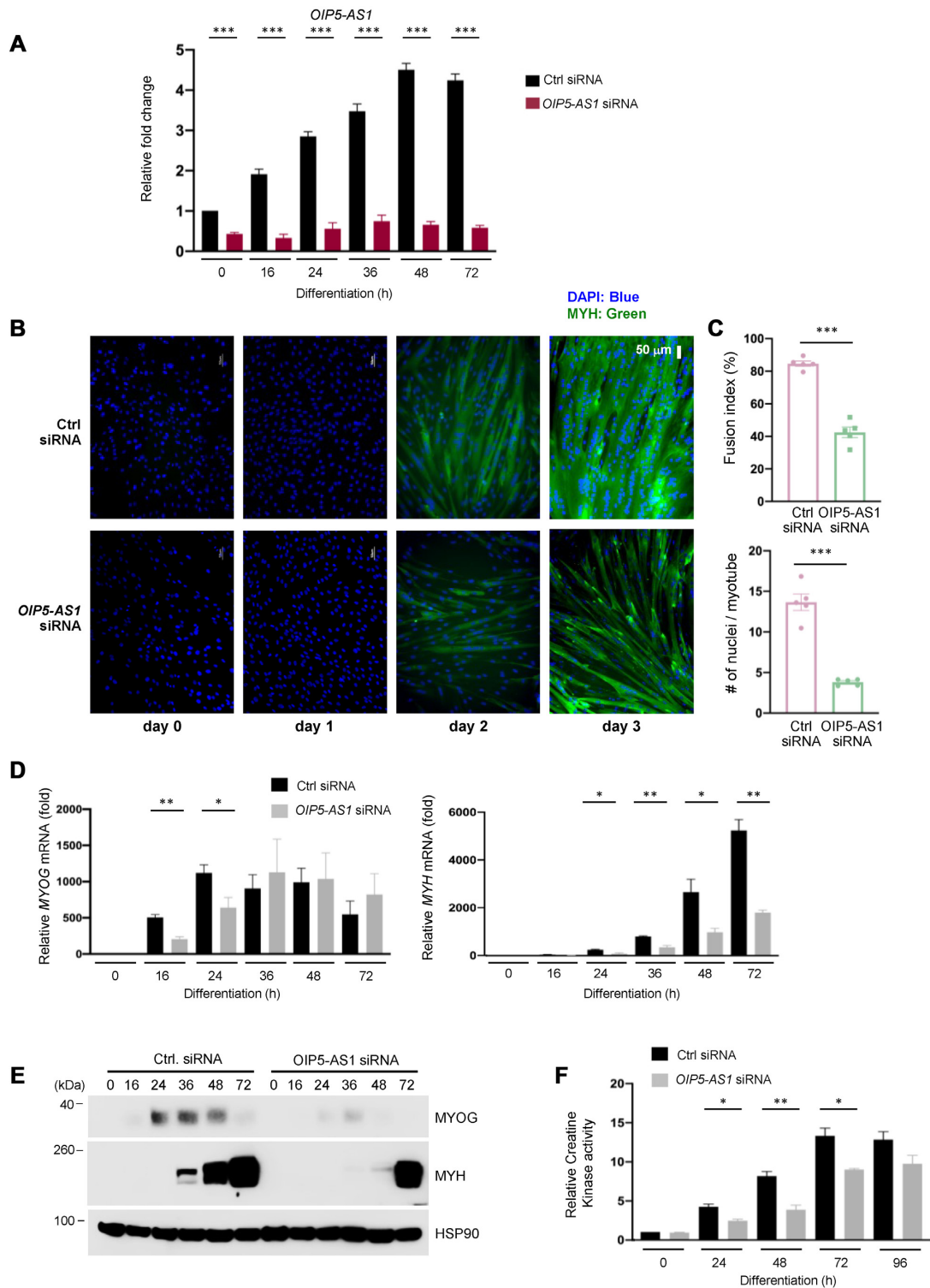


Figure 2. Silencing *OIP5-AS1* attenuates myogenesis. (A) AB1167 myoblasts were transfected with Ctrl siRNA or *OIP5-AS1*-directed siRNA #1; 24 h later, they were placed in differentiation media, and collected at the times shown after the induction of differentiation. The levels of *OIP5-AS1* were measured by RT-qPCR analysis. (B) AB1167 myoblasts were transfected with Ctrl siRNA or *OIP5-AS1*-directed siRNA #1 as described in panel (A), and differentiation was monitored by assessing MYH levels by immunofluorescence at the times indicated. (C) AB1167 myoblasts were transfected with Ctrl siRNA or *OIP5-AS1*-directed siRNA #1 as described in panel (A), and after differentiation for 2 days, the fusion index and the number of nuclei per myotube were quantified; five fields were assessed per experiment. (D) The levels of *MYOG*, *MYOD*, and *MYH* mRNAs were assessed in AB1167 cells transfected as in panel (A). (E) The levels of *MYOG*, *MYOD*, *MYH*, and loading control HSP90 were assessed by western blot analysis in AB1167 myoblasts transfected as in (A) Ctrl or *OIP5-AS1*-directed siRNA #1 and collected at the times shown after the induction of differentiation. (F) The levels of creatine kinase activity were assessed in cells transfected as in panel (A). Data in (A, C, E) are the means \pm SEM from three or more biological replicates. Significance was established using Student's *t*-test. **P* < 0.05; ***P* < 0.01; ****P* < 0.001. Other data are representative of three or more biological replicates.

***OIP5-AS1* partially complements *MEF2C* 3'UTR and promotes *MEF2C* mRNA stability**

LncRNAs can play diverse roles in cellular events by interacting with multiple molecular partners including DNA, RNA, and protein (1,3). Cytoplasmic lncRNAs may have additional functions through interactions with other RNAs as well as with proteins (25). Given that *OIP5-AS1* was primarily localized in the cytoplasm during myogenesis (Supplementary Figure S4A) and was recently found to interact with a range of mRNAs (26), we tested systematically if *OIP5-AS1* was capable of associating with mRNAs encoding myogenic proteins, including MYH and myogenic regulatory factors (MYOD, MYOG and members of the MEF2 family). As shown in Figure 3A, using biotinylated Antisense Oligonucleotides (ASOs) to pull down *OIP5-AS1* from AB1167 cell lysates, only *MEF2C* mRNA was enriched in the pulldown material while other myogenic mRNAs were not. BLAST survey analysis identified nine sites of complementarity between *OIP5-AS1* and *MEF2C* mRNA. Notably, eight of these sequences were located in the *MEF2C* 3' untranslated region (UTR) and only one site was present in the coding region (Figure 3B).

This interaction appeared to be important for the production of MEF2C, as silencing *OIP5-AS1* in AB1167 myoblasts not only delayed myogenic differentiation (Figure 2), but it also reduced the levels of *MEF2C* mRNA and MEF2C protein (Figure 4A). To investigate whether *OIP5-AS1* regulated *MEF2C* mRNA levels by binding specifically to the *MEF2C* 3'UTR, we generated constructs spanning different segments of the *MEF2C* 3'UTR. As shown in Figure 4B, luciferase constructs were prepared in which the renilla luciferase (*RL*) coding region was linked to fragments I, II or III (containing 1, 3 or 4 potential binding sites, respectively); the psiCHECK2 vector also encodes the firefly luciferase (*FL*) gene used to normalize the luciferase results and control for transfection. After transfection of the constructs into AB1167 myoblasts and induction of differentiation for 24 h, only fragment II, but not fragments I or III, increased luciferase activity significantly (Figure 4C), indicating that fragment II contains *MEF2C* sequences that promote luciferase production. In addition, the levels of *RL* mRNA relative to *FL* mRNA followed the same trend, indicating that the rise in luciferase activity was due to a relative increase in the levels of *FL* mRNA and not to changes in translation or luciferase activity (Supplementary Figure S4B). Importantly, *OIP5-AS1* contributed to the rise in expression driven by fragment II, as silencing *OIP5-AS1* lowered the luciferase activity that had been enhanced by *MEF2C* 3'UTR fragment II (Figure 4D). These findings implicated *OIP5-AS1* in promoting MEF2C production through the *MEF2C* 3'UTR fragment II.

To map more precisely the functional sites of *OIP5-AS1* interaction with *MEF2C* 3' UTR fragment II, we sequentially deleted sequences in fragment II. As shown in Figure 4E, loss of the putative binding site 3 was sufficient to fully suppress reporter activity, suggesting that *OIP5-AS1*-complementary site 3 located in fragment II (Figure 4B) was important for promoting reporter expression. To test this hypothesis directly, we deleted complementarity fragment II-3 (21 nucleotides) of *MEF2C* 3'UTR, creating a reporter that

had fragment II but with region 3 deleted, *MEF2C* 3'UTR II-3 Δ . This deletion reporter exhibited significantly reduced luciferase activity than the reporter with the wild-type fragment II (Figure 4F), confirming the importance of complementary site 3 in the *MEF2C* 3'UTR fragment II for the enhanced luciferase expression.

We tested the interaction between these two RNAs in an additional way. Among the transcript variants of *OIP5-AS1* expressed in myoblasts, the 1.9-kb *OIP5-AS1* [NR_026757.1, studied in (16) and fully contained in the longest and most abundant, 8.8-kb *OIP5-AS1* variant (not shown)] contained the region of complementarity with *MEF2C* 3'UTR fragment II-3. We prepared a construct that expressed *OIP5-AS1(s)* tagged with MS2 RNA hairpins (24 total) *OIP5-AS1-MS2*, which was verified to have a similar localization as the endogenous *OIP5-AS1* (Supplementary Figure S4D). We co-expressed *OIP5-AS1(s)-MS2* in AB1167 myoblasts with another construct that expressed a fusion protein (MS2-GST) that binds MS2 RNA hairpins and could be pulled down using GSH-containing beads (Figure 4G, schematic). As shown in Figure 4G, using lysates from transfected myoblasts, *OIP5-AS1(s)-MS2* was effectively pulled down using GSH beads (Figure 4G, left graph); importantly, *MEF2C* mRNA was markedly enriched in this pulldown material (Figure 4G, right graph). Pulldown analysis indicated that *OIP5-AS1-MS2* was able to interact with *MEF2C* 3'UTR fragment II, while this interaction was dramatically reduced when testing the deletion mutant transcript *MEF2C* 3'UTR II-3 Δ (Figure 4H and Supplementary Figure S4C). Collectively, these findings support the notion that the *OIP5-AS1* lncRNA and *MEF2C* mRNA interact in myoblasts through complementary sequences located in *OIP5-AS1* and the proximal region (segment II-3) of *MEF2C* 3'UTR. Of note, while 8 *MEF2C* mRNA isoforms differing in the 3'UTR have been described, region 3 of complementarity with *OIP5-AS1* was conserved among all of these isoforms (Supplementary Figure S4E).

To further investigate how *OIP5-AS1* promoted expression of the reporter *RL* mRNA bearing *MEF2C* 3'UTR segment II, we tested the impact of *OIP5-AS1* abundance on *MEF2C* mRNA stability. As shown, endogenous *MEF2C* mRNA levels were reduced constitutively when *OIP5-AS1* was silenced (Figure 4I, left). We then measured the half-life of *MEF2C* mRNA by blocking *de novo* transcription using actinomycin D and measuring the time required for *MEF2C* mRNA to reach one-half the abundance measured at time 0. As shown, the half-life of *MEF2C* mRNA declined markedly faster in AB1167 myoblasts in which *OIP5-AS1* was silenced ($t_{1/2} \sim 5$ h) compared to control cells ($t_{1/2} > 10$ h) (Figure 4I, right). As a control, a stable transcript, *GAPDH* mRNA (encoding the housekeeping protein GAPDH), showed comparable half-lives whether *OIP5-AS1* was silenced or not. In keeping with the higher levels of *OIP5-AS1* in late myogenesis, the stability of *MEF2C* mRNA was also higher in myoblasts differentiating for 24 h (Figure 4J, right). These findings indicate that *OIP5-AS1* promotes MEF2C expression during myogenesis by associating with, and stabilizing, *MEF2C* mRNA.

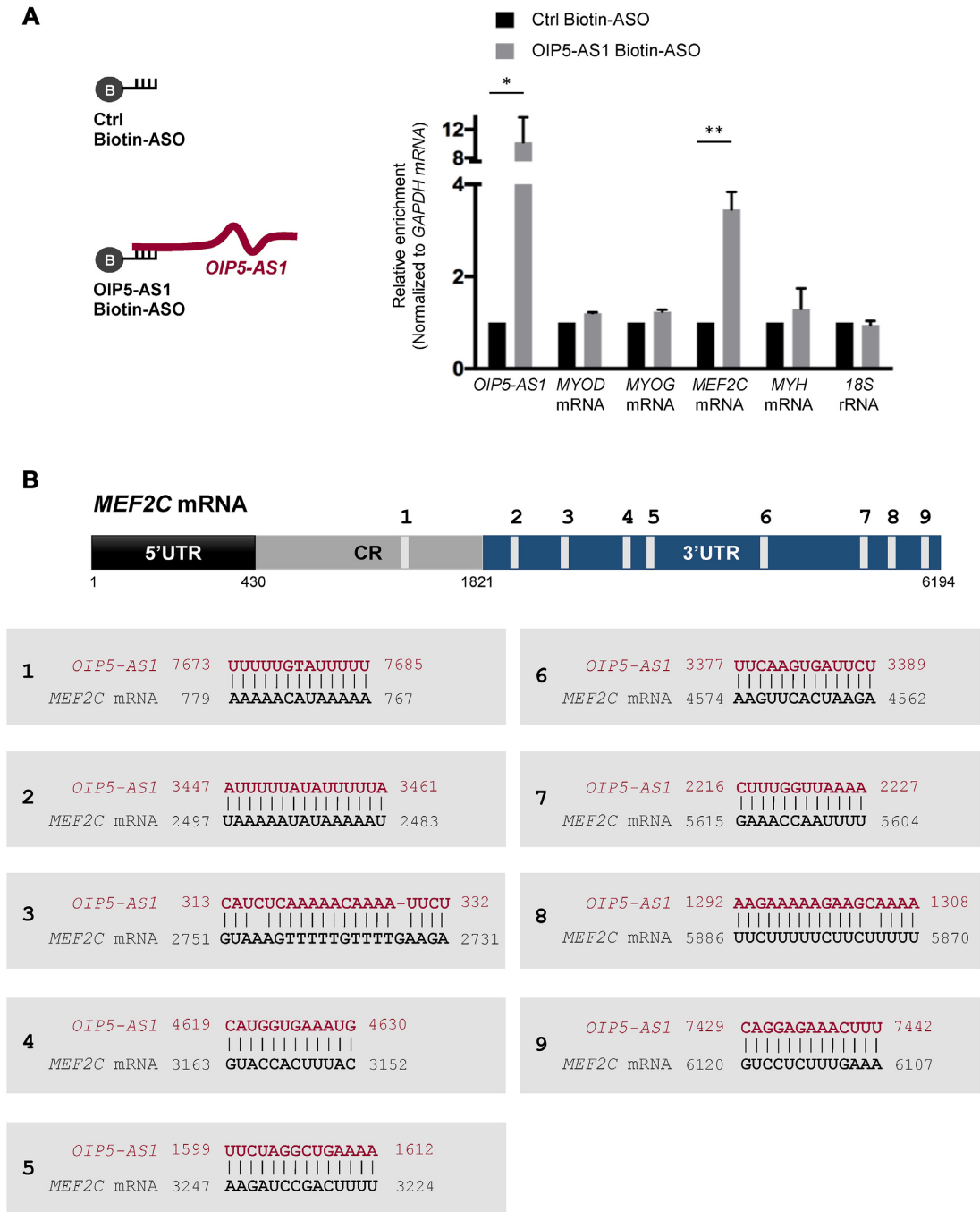


Figure 3. *OIP5-AS1* binds to and shares partial complementarity with *MEF2C* 3'UTR. (A) Left, schematic of biotinylated Ctrl and *OIP5-AS1*-directed ASOs. Right, after incubation of biotinylated ASOs with AB1167 lysates prepared 24 h after inducing differentiation, RNA complexes were pulled down using streptavidin beads (Materials and Methods). The presence of *OIP5-AS1* and myogenesis-related mRNAs in the pull-down material was assessed by RT-qPCR analysis. The levels of test RNAs in the pull-down were normalized to the levels of *GAPDH* mRNA in the lysates. Data in (A,C,E) are the means \pm SEM from three or more biological replicates. Significance was established using Student's *t*-test. **P* < 0.05; ***P* < 0.01; ****P* < 0.001. (B) Regions of potential complementarity identified between *OIP5-AS1* and *MEF2C* mRNA.

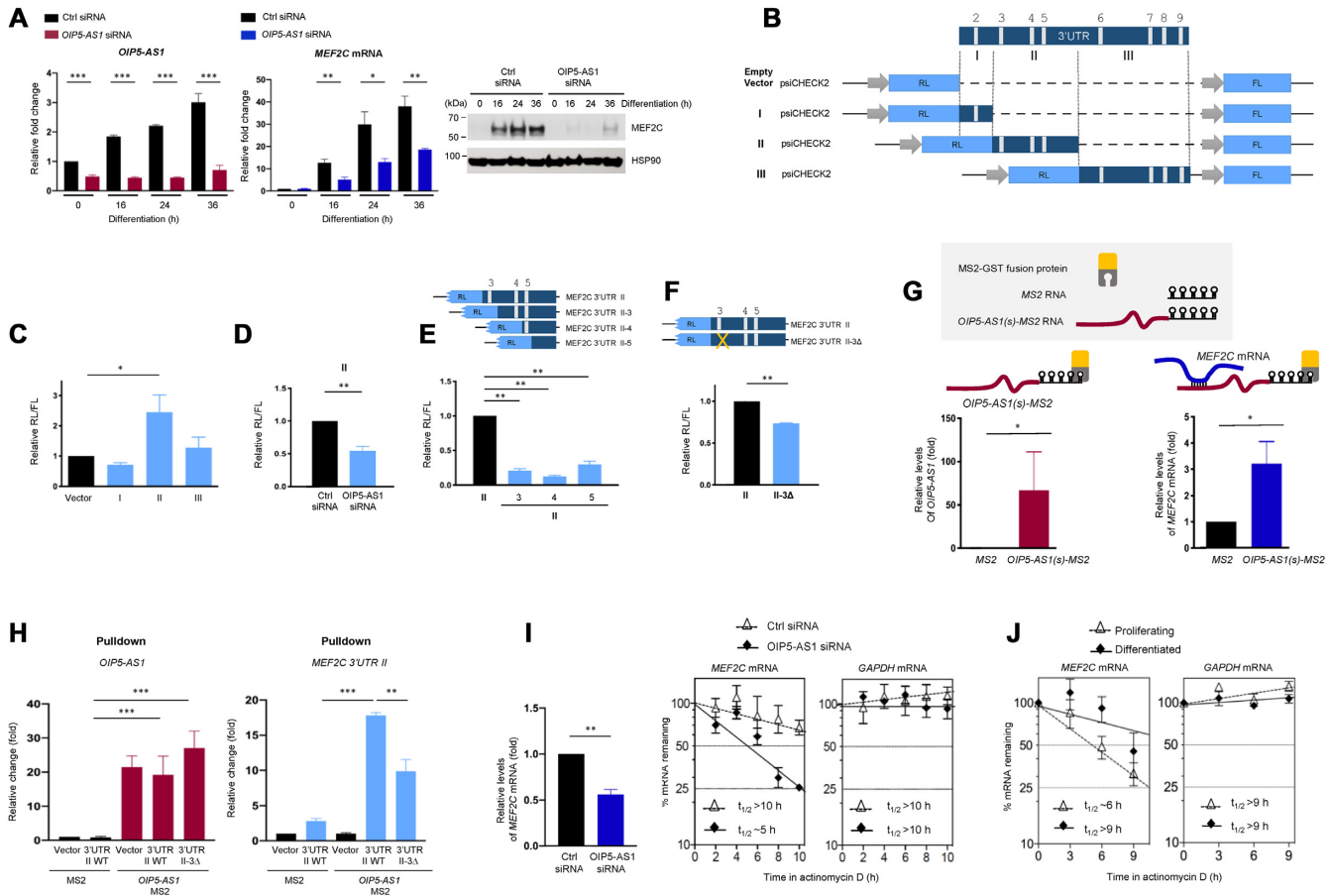


Figure 4. Silencing *OIP5-AS1* lowers MEF2C abundance by diminishing its RNA stability. (A) The levels of *MEF2C* mRNA (top) and MEF2C (bottom) in AB1167 myoblasts transfected with Ctrl or *OIP5-AS1*-directed siRNA #1 and processed as explained in Figure 2A were measured by RT-qPCR analysis (normalized to *GAPDH* mRNA) and western blot analysis (using HSP90 to monitor loading), respectively. (B) Schematic of the psiCHECK2 dual renilla luciferase (RL) and internal control firefly luciferase (FL) reporter constructs used to identify the region(s) of *MEF2C* 3'UTR regulated by *OIP5-AS1*. (C) Twenty-four hours after transfecting the plasmids shown, bearing *MEF2C* 3'UTR regions I, II, and III, AB1167 myoblasts were induced to differentiate for 24 h, and the relative RL/FL ratios were determined. (D) AB1167 myoblasts were co-transfected with *MEF2C* 3'UTR fragment II, along with either Ctrl siRNA or *OIP5-AS1* siRNA; 24 h later they were replaced with differentiation media and cultured for an additional 24 h. The relative RL/FL ratios were determined. (E) AB1167 myoblasts were co-transfected with subsegments II-3, II-4 or II-5 of *MEF2C* 3'UTR fragment II; 24 h later they were replaced with differentiation media and cultured for an additional 24 h, whereupon the relative RL/FL ratios were determined. (F) AB1167 myoblasts were co-transfected with *MEF2C* 3'UTR fragment II or with fragment II lacking site 3 of interaction with *OIP5-AS1* (II-3Δ); 24 h later they were replaced with differentiation media and cultured for an additional 24 h, whereupon the relative RL/FL ratios were determined. (G) Schematic of the MS2 pull-down assay, including plasmids pMS2 (a control vector expressing MS2 RNA), pOIP5-AS1(s)-MS2 (a vector expressing the chimeric RNA *OIP5-AS1*-MS2) and pMS2-GST, expressing a fusion protein (MS2-GST) which recognizes MS2 RNA tags and can be pulled down using glutathione (GSH) beads. Twenty-four hours after transfecting AB1167 myoblasts with either pMS2 or pOIP5-AS1(s)-MS2, as well as with pMS2-GST, cells were induced to differentiate. Twenty-four hours later, cell lysates were analyzed by pull-down using GSH-conjugated beads. The relative interaction of MS2 and *OIP5-AS1*(s)-MS2 with *MEF2C* mRNA was assessed by RT-qPCR analysis. (H) Twenty-four hours after transfecting plasmids expressing *MEF2C* 3'UTR fragment II or *MEF2C* 3'UTR fragment II-3Δ, or an empty vector control plasmid into AB1167 myoblasts, together with plasmids pMS2 or pOIP5-AS1(s)-MS2, as well as with pMS2-GST, cells were induced to differentiate. Twenty-four hours later, cell lysates were analyzed by pull-down using GSH-conjugated beads. The relative interaction of MS2 and *OIP5-AS1*-MS2 with *MEF2C* 3'UTR fragment II or *MEF2C* 3'UTR fragment II-3Δ was assessed by RT-qPCR analysis of the pull-down materials. (I) Twenty-four hours after transfecting Ctrl or *OIP5-AS1* siRNAs, AB1167 myoblasts were placed in differentiation media for an additional 24 h, whereupon the steady-state levels of *MEF2C* mRNA were quantified (left). Cells were then treated with actinomycin D and the relative levels of *MEF2C* mRNA and normalization control transcript *GAPDH* mRNA were assessed by RT-qPCR analysis and normalized to 18S rRNA levels, also quantified by RT-qPCR analysis (right). mRNA half-lives ($t_{1/2}$) were calculated as the times required to reach 50% of the initial abundance of the mRNA at time 0 before adding actinomycin D. (J) AB1167 myoblasts that were either proliferating or induced to differentiate for 24 h were treated with actinomycin D to measure the stability of *MEF2C* mRNA as explained in panel (I). In panels (A, C–J) the data represent the means \pm SEM from three or more independent experiments. Significance was established using Student's *t*-test. * $P < 0.05$; ** $P < 0.01$; *** $P < 0.001$. Data in (A) are representative of three or more biological replicates.

***OIP5-ASI* recruits HuR to *MEF2C* mRNA, enhances *MEF2C* mRNA stability**

We sought to gain insight into the mechanisms leading to *MEF2C* mRNA stabilization by *OIP5-ASI*. We surveyed RNA-binding proteins (RBPs) that might associate with both transcripts and promote mRNA stability (27). Using the POSTAR2 database, a number of RBPs were found by PAR-CLIP (photoactivatable ribonucleoside-enhanced crosslinking and immunoprecipitation) analysis to associate with *MEF2C* mRNA and with *OIP5-ASI* (28,29), but only three RBPs—HuR/ELAVL1, WDR23 and CSTF2T—associated with both RNAs (Figure 5A). HuR was previously reported to associate with *OIP5-ASI* and *MEF2C* mRNA (16,30), so we hypothesized that HuR may be a key mediator of the actions of *OIP5-ASI* in stabilizing *MEF2C* mRNA.

We examined if HuR interacted with *OIP5-ASI* in myoblasts using a range of methods. We performed RIP (ribonucleoprotein immunoprecipitation) analysis with an anti-HuR antibody and lysates prepared from differentiated AB1167 myoblasts using IP conditions that preserved ribonucleoprotein (RNP) complexes. After isolating RNA from the RNPs present in the IP material, the levels of *OIP5-ASI*, as detected using RT-qPCR analysis, were highly enriched in the HuR IP (Figure 5B, left), supporting the existence of these complexes in AB1167 myoblasts. We then employed *OIP5-ASI*-directed ASOs to pull down and identify interacting proteins; here too, *OIP5-ASI* pulled down HuR far more effectively than a control (Ctrl) ASO (Figure 5B, middle). Finally, we tested the ability of HuR to associate with tagged *OIP5-ASI(s)-MS2* RNA in AB1167 myoblasts co-expressing the GST-MS2 fusion protein; pull-down analysis revealed a similarly strong enrichment of HuR associated with the *OIP5-ASI-MS2* relative to levels observed with a control *MS2* RNA (Figure 5B, right).

Turning our attention to *MEF2C* mRNA, RIP analysis verified that *MEF2C* mRNA was capable of binding HuR (Figure 5C, left). In keeping with the ability of HuR to modulate the turnover and translation of many target mRNAs (31), silencing HuR in differentiated AB1167 myoblasts for 48 h reduced the levels of *MEF2C* mRNA and MEF2C protein, as determined by RT-qPCR and western blot analyses, respectively (Figure 5D, E), while reduced HuR expression did not affect *OIP5-ASI* levels in AB1167 cells (Figure 5F). Interestingly, however, actinomycin D treatment revealed that HuR was required for stabilizing *MEF2C* mRNA, as silencing HuR reduced the half-life to ~10 h (Figure 5F). Thus, we hypothesized that *OIP5-ASI* and HuR might jointly regulate *MEF2C* mRNA stability. To test this possibility, we silenced *OIP5-ASI* in HEK293 cells and monitored the interaction of HuR with *MEF2C* mRNA. Silencing *OIP5-ASI* did not affect HuR levels (Figure 5G), but it significantly reduced the interaction of HuR with *MEF2C* mRNA (Figure 5H, left). This reduction in binding was specific for *MEF2C* mRNA, as other HuR targets like *MMP9* mRNA, which does not have *OIP5-ASI* complementarity sites, showed comparable binding to HuR regardless of *OIP5-ASI* abundance (Figure 5H, right). These results indicate that HuR binds both *MEF2C* mRNA and *OIP5-ASI* lncRNA, and that *MEF2C* mRNA stabilization leading to

MEF2C protein production requires the presence of both *OIP5-ASI* and HuR.

***OIP5-ASI* is required for HuR-*MEF2C* mRNA interaction**

To study if the promotion of human skeletal myogenic differentiation by *OIP5-ASI* was linked to the enhanced production of MEF2C, we carried out a number of rescue experiments. A construct was made to express myc-tagged MEF2C protein from an mRNA that lacked 3'UTR and hence did not have *OIP5-ASI*-interacting sites. After transfection of the vector into AB1167 myoblasts, exogenous MEF2C-myc and endogenous MEF2C proteins were detected by western blot analysis (Figure 6A). Silencing *OIP5-ASI* reduced the levels of endogenous MEF2C, in keeping with the finding that silencing *OIP5-ASI* lowered *MEF2C* mRNA levels and *MEF2C* mRNA stability (Figure 4H); importantly, however, overexpression of MEF2C-myc partially restored myogenesis as measured by the increased levels of MYH and creatine kinase activity, as well as by the elevated myotube formation (Figure 6A and Supplementary Figure S5A).

Similarly, the reduction in myogenesis elicited by silencing *OIP5-ASI* [in this instance using an siRNA that was directed at the distal region of *OIP5-ASI*, outside of the region ectopically expressed, *OIP5-ASI(s)*], evidenced by a loss of MEF2C protein levels and reduced creatine kinase activity (Figure 6B), was rescued by ectopic overexpression of the short *OIP5-ASI(s)* that bears the region of complementarity with *MEF2C* 3'UTR segment II-3 (Figure 6B). Importantly, however, ectopically expressing *OIP5-ASI(s)Δ*, which lacks the region that complements *MEF2C* 3'UTR segment II-3 and hence has reduced ability to bind *MEF2C* mRNA (Supplementary Figure S5B), did not rescue MEF2C protein production or creatine kinase activity (Figure 6B). Taken together, our findings support a model whereby the lncRNA *OIP5-ASI*, which is highly expressed in muscle and is elevated during myogenesis, functions as an interactive scaffold to recruit the RBP HuR for binding to the *MEF2C* 3'UTR, in turn stabilizing *MEF2C* mRNA and promoting MEF2C expression and myogenic differentiation (Figure 6C).

DISCUSSION

Muscle development and regeneration are tightly orchestrated through the strict coordination of gene expression programs. Myogenesis is regulated by major transcription factors, such as MYF5, MYOD, MYOG and MRF4 (4,32), as well as by a growing number of RBPs and noncoding RNAs (11,33). Here, we have identified *OIP5-ASI*, a human lncRNA highly expressed in muscle, as a major regulator of human myogenesis that appeared to be functionally important, as silencing *OIP5-ASI* attenuated myogenesis and delayed myotube formation. Molecular details of this regulation were uncovered through the identification of *MEF2C* mRNA as a transcript that was partially complementary to *OIP5-ASI* and was stabilized through its association with *OIP5-ASI*. Interestingly, this lncRNA-mRNA interaction facilitated HuR binding to *MEF2C* mRNA, leading to *MEF2C* mRNA stabilization and increased MEF2C

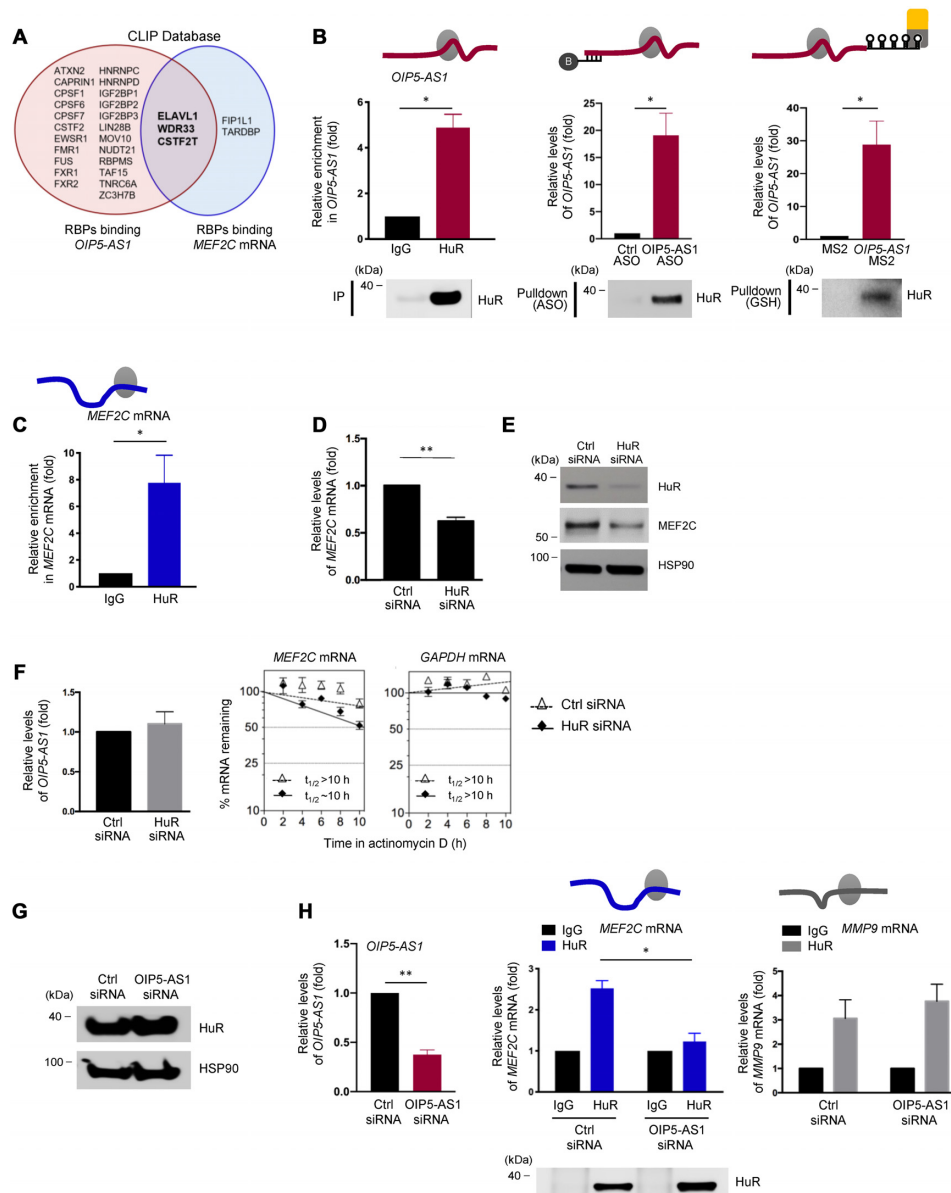


Figure 5. HuR binds *OIP5-AS1* and *MEF2C* mRNA, stabilizes *MEF2C* mRNA. (A) Venn diagram of RBPs from the CLIP database (Materials and Methods) binding *OIP5-AS1* (red) and those binding *MEF2C* mRNA (blue); 3 RBPs binding both RNAs are listed in the intersection. (B) Binding of HuR to *OIP5-AS1* in differentiated AB1167 cultures was verified by HuR RNP immunoprecipitation (RIP) analysis (left); after HuR RIP (Materials and Methods) using IgG or anti-HuR antibodies, the presence of *OIP5-AS1* in the IP materials was measured by RT-qPCR analysis, normalized to the levels of *GAPDH* mRNA (a transcript that is not a target of HuR), and represented as the enrichment of *OIP5-AS1* in HuR IP relative to the levels in IgG IP. Western blot analysis was performed to monitor the efficiency of the HuR IP reaction. For *OIP5-AS1* pull-down analysis (middle), differentiated AB1167 cultures were incubated with biotin-ASO-conjugated *OIP5-AS1*; HuR bound to the *OIP5-AS1* ASO was detected by western blot analysis. A control (Ctrl) ASO was used to detect background binding of HuR. RT-qPCR analysis was performed to monitor the efficiency of the *OIP5-AS1* pull-down. Further validation of this interaction was gained by assaying HuR binding to *OIP5-AS1-MS2* (right); lysates prepared from differentiated AB1167 cultures expressing *OIP5-AS1-MS2* or *MS2* along with GST-MS2-binding protein (as described in Figure 4G) were subjected to western blot analysis to detect HuR in the GST pull-down material. Input, aliquots of the lysates before pull-down. RT-qPCR analysis was performed to monitor the efficiency of *OIP5-AS1-MS2* pull-down. (C) HuR RIP analysis was performed as described in panel (B), and the presence of *MEF2C* mRNA was quantified by RT-qPCR analysis. (D-F) Twenty-four hours after transfecting Ctrl or HuR siRNAs, AB1167 myoblasts were differentiated for an additional 24 h and the steady-state levels of *MEF2C* mRNA (D) and MEF2C (E) were determined by RT-qPCR and western blot analyses, respectively. In these transfection groups, the steady-state levels of *OIP5-AS1* were assessed by RT-qPCR analysis (F, left), and the half-life of *MEF2C* mRNA was measured after incubation with actinomycin D, as explained in Figure 4H (F, right). (G, H) Forty-eight hours after transfecting human embryonic kidney fibroblasts (HEK293 cells) with Ctrl siRNA or *OIP5-AS1* siRNA, the levels of HuR were assessed by western blot analysis (G). The relative levels of *OIP5-AS1* were shown by RT-qPCR analysis (H, left), and the binding of HuR to *MEF2C* mRNA was assessed by RIP analysis; data were normalized to the levels of *GAPDH* mRNA in each IP sample and represented as the enrichment of each mRNA relative to the levels in IgG IP (H, middle). *MMP9* mRNA, a target of HuR lacking complementarity to *OIP5-AS1*, was included as control in RIP analyses; as shown, *MMP9* mRNA remained enriched in HuR RIP regardless of *OIP5-AS1* abundance (H, right). Western blot analysis was performed to monitor the efficiency of HuR IP. Data in (B-D,F,H) represent the means \pm SEM from at least three independent experiments. Significance was established using Student's *t*-test. **P* < 0.05; ***P* < 0.01; ****P* < 0.001. Other data are representative of three or more biological replicates.

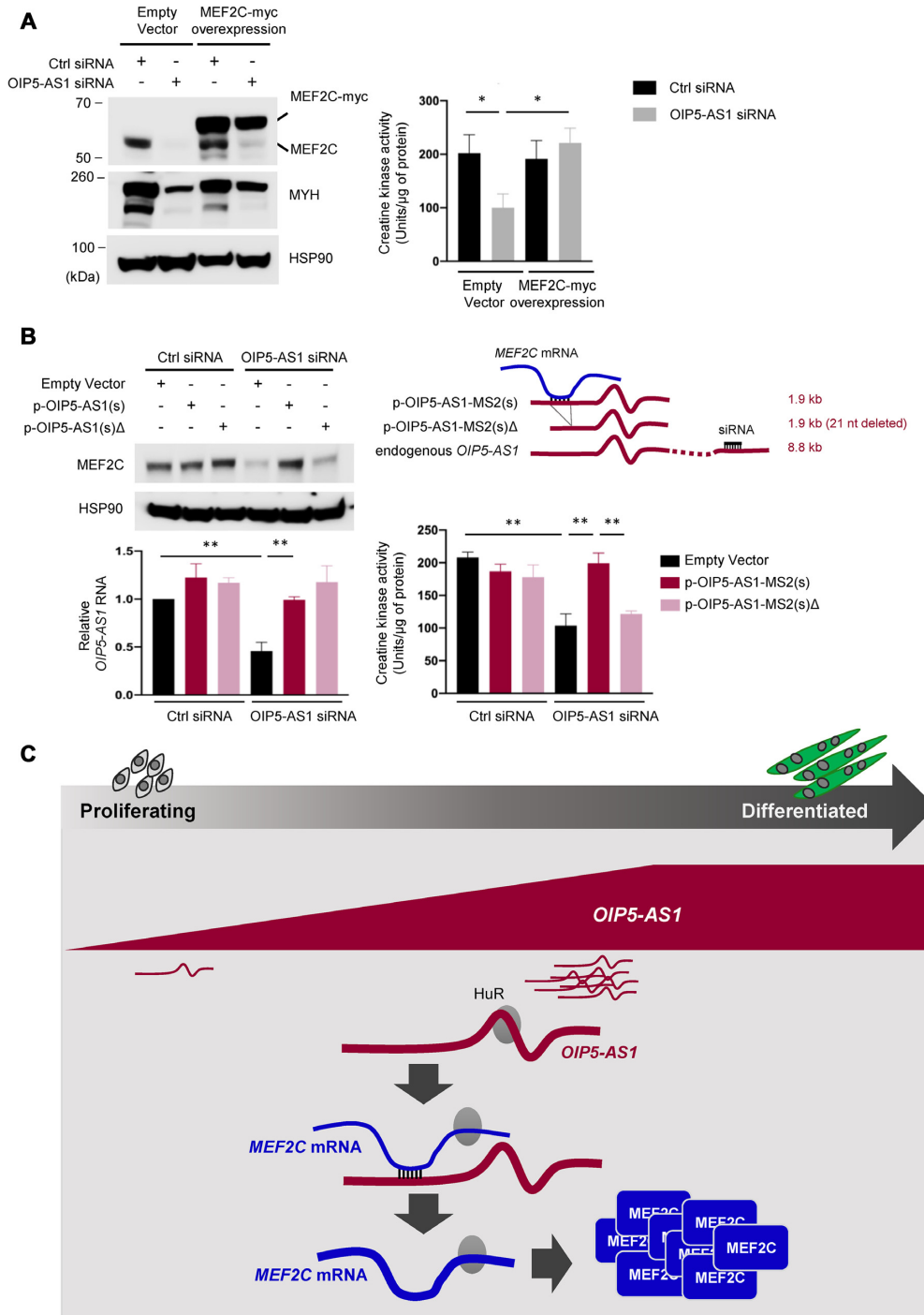


Figure 6. Rescue of myogenesis after silencing *OIP5-AS1* by ectopic MEF2C expression. (A) AB1167 myoblasts were cotransfected with siRNAs (Ctrl or *OIP5-AS1*-directed) and with plasmids (either an Empty Vector control plasmid or a plasmid expressing myc-tagged MEF2C). Twenty-four hours after transfection, AB1167 myoblasts were induced to differentiate and 48 h after that the levels of MEF2C, MEF2C-myc, MYH, and HSP90 were determined by western blot analysis (left), and the activity of the myogenic differentiation marker creatine kinase was measured (right). (B) AB1167 myoblasts were cotransfected with siRNAs (Ctrl or *OIP5-AS1*-directed) and with one of these plasmids: MS2 only control plasmid, a plasmid expressing the short variant of *OIP5-AS1-MS2(s)* that bears the *MEF2C* 3'UTR interacting segment '(s)', or the short variant of *OIP5-AS1-MS2(s)Δ* lacking the *MEF2C* 3'UTR interacting segment, '(s)Δ' (schematic, top right). The endogenous (longer) *OIP5-AS1* transcript depicting the siRNA recognition site outside of the segment in the ectopic vectors is indicated. In these transfection groups, the abundance of MEF2C was assessed by western blot analysis (left top), the levels of *OIP5-AS1* by RT-qPCR analysis (left graph), and the activity of creatine kinase was measured (right graph). (C) Proposed model. In Proliferating (undifferentiated) myoblasts, lncRNA *OIP5-AS1* levels are low. As myogenic differentiation progresses, *OIP5-AS1* levels rise and through its complementarity with *MEF2C* mRNA, it helps recruit HuR to the *MEF2C* 3'UTR and enhances *MEF2C* mRNA stability and MEF2C production. Through this mechanism, *OIP5-AS1* promotes MEF2C expression and enhances myogenesis. Data in (A,B) represent the means ± SEM from at least three independent biological replicates. Significance was established using Student's *t*-test. **P* < 0.05; ***P* < 0.01; ****P* < 0.001. Other data are representative of three or more biological replicates.

production in myoblasts. Conversely, loss of *OIP5-AS1* prevented the timely accumulation of MEF2C and delayed myogenesis. In this paradigm, we propose that the lncRNA *OIP5-AS1* functions to recruit HuR locally to *MEF2C* mRNA, ultimately promoting myogenesis.

LncRNA–mRNA binding

Interactions between a lncRNA and an mRNA have been reported to control mRNA stability and translation. For example, mRNA turnover is controlled by the interaction of 1/2-sbsRNAs with mRNAs, with the double-stranded RNA-binding protein STAU1 (Staufen1) then inducing decay of the target mRNA (34). Another example is offered by *BACE1-AS*, which was shown to bind and stabilize *BACE1* mRNA, encoding β -secretase, an enzyme important for generating the amyloid peptide A β 42 (35,36). As examples of translational control, *lincRNA-p21* partially complemented *CTNNB1* mRNA and *JUNB* mRNA and recruited translational suppressors RCK/p54 and FMRP, lowering the translation of CTNNB1 and JUNB (37), *7SL* RNA bound to *TP53* 3'UTR and repressed its translation by competing with HuR (38). In addition, the antisense lncRNA *Uchl1-AS1* was capable of binding to the *Uchl1* mRNA 5'UTR leading to increased translation of the protein UCHL1 (39). However, to our knowledge, the paradigm described here is the first example of a lncRNA (*OIP5-AS1*) recruiting an RBP to an unrelated mRNA (*MEF2C* 3'UTR) in order to enhance mRNA stability. In this instance, the positive impact of *OIP5-AS1* on the expression of *MEF2C* mRNA led to enhanced skeletal muscle differentiation.

Many regulatory RBPs bind specific RNA sequences, although this binding is typically more flexible than that observed for DNA-binding proteins. In fact, only a small proportion of RNA sites for putative interaction with RBPs are occupied at a given point in time in cells (40), even though many RBPs are in excess. Thus, additional factors such as post-translational modifications of RBPs, local RNA secondary structure, and subcellular compartmentalization of the RNA or the RBP can influence the formation of RNPs (41–43). We propose that the interaction of *OIP5-AS1* with the *MEF2C* 3'UTR through lncRNA–mRNA base pairing might modulate the *MEF2C* 3'UTR RNA structure to promote RBP binding. We further postulate that lncRNA *OIP5-AS1*, which binds HuR at multiple sites, can increase the local concentration of HuR within the cell; then, by specifically interacting with other RNAs such as *MEF2C* mRNA, *OIP5-AS1* facilitates the formation of other HuR RNP complexes. As this work progresses, it will be interesting to expand the analysis and test if *OIP5-AS1* might interact with other mRNAs during myogenesis and facilitate their association with HuR.

HuR RNPs in myogenesis

A survey of RBPs interacting with *OIP5-AS1* revealed that *OIP5-AS1* can associate with other RBPs besides HuR, including hnRNP and FMR1. In cancer cells, *OIP5-AS1* can bind to HuR and reduce the binding of HuR to mRNAs encoding proliferative proteins such as CCND1 and

CCNA2 (cyclins D1 and A2), and in this manner, *OIP5-AS1* can contribute to the reduced proliferation of cancer cells (16). Here, we found that *OIP5-AS1* binding to the *MEF2C* 3'UTR led to *MEF2C* mRNA stabilization and promoted myogenic differentiation. Whether *OIP5-AS1* also contributes to reducing myoblast proliferation to establish the fully differentiated state that favors myogenesis remains to be investigated. It is important to note that in early stages of myogenic differentiation, HuR was shown to bind to mRNAs encoding MYOD and MYOG and p21/CDKN1A, enhancing their early production during myogenesis and helping to establish the first steps in differentiation (9,10). Perhaps the subsequent rise in *OIP5-AS1* helps to redirect HuR to other target mRNAs that must be translated later during the differentiation process, including *MEF2C* mRNA. We propose that HuR supports different stages of myogenesis by participating in different mRNPs and lncRNPs, as shown for the long intergenic noncoding RNA *linc-MD1* (44,45). It is important to note that the existence of many other factors capable of binding *OIP5-AS1* and HuR helps to explain why the reduction of *MEF2C* mRNA stability seen after silencing HuR (Figure 5F) is different in magnitude from that seen after silencing *OIP5-AS1* (Figure 4I). The mechanisms that regulate the increased *OIP5-AS1* levels during myogenesis are not known, but the fact that the precursor transcript (*pre-OIP5-AS1*) increases during myogenesis (Supplementary Figure S6C) suggests that this elevation is at least in part due to enhanced transcription. Whether myogenic factors control *OIP5-AS1* transcription also remains to be studied.

Local conservation of *OIP5-AS1*

While overall lncRNA sequences are poorly conserved among species, secondary structures, partial sequences, and interactions with molecular partners (e.g., miRNAs and RBPs) are more conserved. In this regard, *OIP5-AS1* is not highly conserved but some segments have been identified as being functionally conserved among species. For example, a miR-7 binding site in *OIP5-AS1* is conserved from zebrafish to human; in this regard, *OIP5-AS1* binds to and regulates miR-7, influencing miR-7 actions in neuronal development of zebrafish and mice (15,18). Here, we found that silencing *OIP5-AS1/Oip5-as1* attenuated both human (AB1167 cells) and mouse (C2C12 cells) myogenesis (Figure 2; Supplementary Figure S6A). *OIP5-AS1* is highly abundant in muscle tissue and interacts abundantly with HuR in both human and mouse myoblasts (Supplementary Figure S6B). Interestingly, the short isoform of *OIP5-AS1*, which appears to be most abundant (Supplementary Figure S6D), also has the highest identity with murine *Oip5-as1*, including several sites complementary to mouse *Mef2c* mRNA and HuR-binding sites. Whether *OIP5-AS1* has a conserved biological role in myogenesis by interacting with HuR and influencing MEF2C production in other species warrants further study.

OIP5-AS1–HuR complexes beyond myogenesis

OIP5-AS1 has also been implicated in cancer. It suppresses cell proliferation by reducing GAK levels, and acts as a

competing endogenous RNA for miR-218 binding to promote Kaposi's sarcoma (17,46). MEF2C is also reported to promote the progression of lung cancer and osteosarcoma (47,48). Given that HuR is highly expressed in numerous cancers and contributes to carcinogenic gene expression programs (31), it will be important to determine if *OIP5-AS1* influences HuR binding to *MEF2C* mRNA or other cancer-associated mRNAs in the context of carcinogenesis.

In closing, the recruitment of lncRNA–RBP complexes to target nucleic acids has been studied in depth in the nucleus, where lncRNAs have been shown to recruit proteins to specific DNA regions to elicit changes in gene transcription. The paradigm presented here, *OIP5-AS1* recruiting HuR to *MEF2C* mRNA to coordinate myogenesis, illustrates a similar process at the post-transcriptional level. Akin to lncRNAs driving *transcriptional* programs, lncRNAs can also drive *post-transcriptional* programs by directing RBPs to subsets of mRNAs, thereby helping to orchestrate complex developmental processes such as myogenesis.

DATA AVAILABILITY

GEO: GSE136004 and GSE92632 (<https://www.ncbi.nlm.nih.gov/geo/>). Images of original blots are included in the Supplementary Figure S7.

SUPPLEMENTARY DATA

Supplementary Data are available at NAR Online.

ACKNOWLEDGEMENTS

This work was supported entirely by the NIA IRP, NIH. We thank V. Raz (Leiden University Medical Centre, The Netherlands) and V. Mouly (INSERM, France) for the human myoblasts.

Author contributions: J.H.Y. and M.G. conceived the study and designed experiments; J.H.Y., M.W.C., P.R.P. and D.T. performed and analyzed experiments; X.Y., J.L.M. and R.M. provided technical support; S.D. performed the bioinformatic analysis; K.A. contributed intellectually; J.H.Y. and M.G. wrote the manuscript.

FUNDING

National Institute on Aging IRP; NIH. Funding for open access charge: National Institute on Aging IRP; NIH.

Conflict of interest statement. None declared.

REFERENCES

- Kopp, F. and Mendell, J.T. (2018) Functional classification and experimental dissection of long noncoding RNAs. *Cell*, **172**, 393–407.
- Noh, J.H., Kim, K.M., McClusky, W.G., Abdelmohsen, K. and Gorospe, M. (2018) Cytoplasmic functions of long noncoding RNAs. *Wiley Interdiscip. Rev. RNA*, **9**, e1471.
- Rinn, J.L. and Chang, H.Y. (2012) Genome regulation by long noncoding RNAs. *Annu. Rev. Biochem.*, **81**, 145–166.
- Bentzinger, C.F., Wang, Y.X. and Rudnicki, M.A. (2012) Building muscle: molecular regulation of myogenesis. *Cold Spring Harbor Persp. Biol.*, **4**, a008342.
- Baracos, V.E., Martin, L., Korc, M., Guttridge, D.C. and Fearon, K.C.H. (2018) Cancer-associated cachexia. *Nature Rev.*, **4**, 17105.
- Marcell, T.J. (2003) Sarcopenia: causes, consequences, and preventions. *J. Gerontol.*, **58**, M911–M916.
- Molkentin, J.D. and Olson, E.N. (1996) Defining the regulatory networks for muscle development. *Curr. Opin. Genet. Dev.*, **6**, 445–453.
- Apponi, L.H., Corbett, A.H. and Pavlath, G.K. (2011) RNA-binding proteins and gene regulation in myogenesis. *Trends Pharmacol. Sci.*, **32**, 652–658.
- Figuerola, A., Cuadrado, A., Fan, J., Atasoy, U., Muscat, G.E., Munoz-Canoves, P., Gorospe, M. and nad Munoz, A. (2003) Role of HuR in skeletal myogenesis through coordinate regulation of muscle differentiation genes. *Mol. Cell. Biol.*, **23**, 4991–5004.
- van der Giessen, K., Di-Marco, S., Clair, E. and Gallouzi, I.E. (2003) RNAi-mediated HuR depletion leads to the inhibition of muscle cell differentiation. *J. Biol. Chem.*, **278**, 47119–47128.
- Ballarino, M., Morlando, M., Fatica, A. and Bozzoni, I. (2016) Non-coding RNAs in muscle differentiation and musculoskeletal disease. *J. Clin. Invest.*, **126**, 2021–2030.
- Cesana, M., Cacchiarelli, D., Legnini, I., Santini, T., Sthandier, O., Chinappi, M., Tramontano, A. and Bozzoni, I. (2011) A long noncoding RNA controls muscle differentiation by functioning as a competing endogenous RNA. *Cell*, **147**, 358–369.
- Gong, C., Li, Z., Ramanujan, K., Clay, I., Zhang, Y., Lemire-Brachat, S. and Glass, D.J. (2015) A long non-coding RNA, LncMyoD, regulates skeletal muscle differentiation by blocking IMP2-mediated mRNA translation. *Dev. Cell*, **34**, 181–191.
- Zhu, M., Liu, J., Xiao, J., Yang, L., Cai, M., Shen, H., Chen, X., Ma, Y., Hu, S., Wang, Z. *et al.* (2017) Lnc-mg is a long non-coding RNA that promotes myogenesis. *Nat. Commun.*, **8**, 14718.
- Ulitsky, I., Shkumatava, A., Jan, C.H., Sive, H. and Bartel, D.P. (2011) Conserved function of lincRNAs in vertebrate embryonic development despite rapid sequence evolution. *Cell*, **147**, 1537–1550.
- Kim, J., Abdelmohsen, K., Yang, X., De, S., Grammatikakis, I., Noh, J.H. and Gorospe, M. (2016) LncRNA *OIP5-AS1/cyano* sponges RNA-binding protein HuR. *Nucleic Acids Res.*, **44**, 2378–2392.
- Kim, J., Noh, J.H., Lee, S.K., Munk, R., Sharov, A., Lehrmann, E., Zhang, Y., Wang, W., Abdelmohsen, K. and Gorospe, M. (2017) LncRNA *OIP5-AS1/cyano* suppresses GAK expression to control mitosis. *Oncotarget*, **8**, 49409–49420.
- Kleaveland, B., Shi, C.Y., Stefano, J. and Bartel, D.P. (2018) A network of noncoding regulatory RNAs acts in the mammalian brain. *Cell*, **174**, 350–362.
- Mamchaoui, K., Trollet, C., Bigot, A., Negroni, E., Chaouch, S., Wolff, A., Kandalla, P.K., Marie, S., Di Santo, J., St Guily, J.L. *et al.* (2011) Immortalized pathological human myoblasts: towards a universal tool for the study of neuromuscular disorders. *Skelet. Muscle*, **1**, 34.
- Kim, K.M., Noh, J.H., Bodogai, M., Martindale, J.L., Yang, X., Indig, F.E., Basu, S.K., Ohnuma, K., Morimoto, C., Johnson, P.F. *et al.* (2017) Identification of senescent cell surface targetable protein DPP4. *Genes Dev.*, **31**, 1529–1534.
- Noh, J.H., Kim, K.M., Abdelmohsen, K., Yoon, J.H., Panda, A.C., Munk, R., Kim, J., Curtis, J., Moad, C.A., Wohler, C.M., Indig, F.E. *et al.* (2016) HuR and GRSF1 modulate the nuclear export and mitochondrial localization of the lncRNA RMRP. *Genes Dev.*, **30**, 1224–1239.
- Ulitsky, I. (2016) Evolution to the rescue: using comparative genomics to understand long non-coding RNAs. *Nat. Rev. Genet.*, **17**, 601–614.
- Pandey, P.R., Yang, J.H., Tsitsipatis, D., Panda, A.C., Noh, J.H., Kim, K.M., Munk, R., Nicholson, T., Hanniford, D., Argibay, D. *et al.* (2020) circSamd4 represses myogenic transcriptional activity of PUR proteins. *Nucleic Acids Res.*, **48**, 3789–3805.
- Bergstrom, D.A., Penn, B.H., Strand, A., Perry, R.L.S., Rudnicki, M.A. and Tapscott, S.J. (2002) Promoter-specific regulation of MyoD binding and signal transduction cooperate to pattern gene expression. *Mol. Cell*, **9**, 587–600.
- Noh, J.H., Kim, K.M., McClusky, W.G., Abdelmohsen, K. and Gorospe, M. (2018) Cytoplasmic functions of long noncoding RNAs. *Wiley Interdiscip. Rev. RNA*, **9**, e1471.
- Zealy, R.W., Fomin, M., Davila, S., Makowsky, D., Thigpen, H., McDowell, C.J., Cummings, J.C., Lee, E.S., Kwon, S.H., Min, K.W. *et al.* (2018) Long noncoding RNA complementarity and target transcripts abundance. *Biochim. Biophys. Acta*, **1861**, 224–234.

27. Hentze, M.W., Castello, A., Schwarzl, T. and Preiss, T. (2018) A brave new world of RNA-binding proteins. *Nat. Rev. Mol. Cell. Biol.*, **19**, 327–341.
28. Yang, Y.C., Di, C., Hu, B., Zhou, M., Liu, Y., Song, N., Li, Y., Umetsu, J. and Lu, Z.J. (2015) CLIPdb: a CLIP-seq database for protein-RNA interactions. *BMC Genomics*, **16**, 51.
29. Zhu, Y., Xu, G., Yang, Y.T., Xu, Z., Chen, X., Shi, B., Xie, D., Lu, Z.J. and Wang, P. (2019) POSTAR2: deciphering the post-transcriptional regulatory logics. *Nucleic Acids Res.*, **47**, D203–D211.
30. Zhou, A., Shi, G., Kang, G.J., Xie, A., Liu, H., Jiang, N., Liu, M., Jeong, E.M. and Dudley, S.C. Jr (2018) RNA binding protein, HuR, regulates SCN5A expression through stabilizing MEF2C transcription factor mRNA. *J. Am. Heart Assoc.*, **7**, e007802.
31. Abdelmohsen, K. and Gorospe, M. (2010) Posttranscriptional regulation of cancer traits by HuR. *Wiley Interdiscip. Rev. RNA*, **1**, 214–229.
32. Bryson-Richardson, R.J. and Currie, P.D. (2008) The genetics of vertebrate myogenesis. *Nat. Rev. Genet.*, **9**, 632–646.
33. Van Pelt, D.W., Hettlinger, Z.R. and Vanderklish, P.W. (2019) RNA-binding proteins: the next step in translating skeletal muscle adaptations? *J. Appl. Physiol.*, **127**, 654–660.
34. Gong, C. and Maquat, L.E. (2011) lncRNAs transactivate STAUI-mediated mRNA decay by duplexing with 3' UTRs via Alu elements. *Nature*, **470**, 284–288.
35. Faghihi, M.A., Modarresi, F., Khalil, A.M., Wood, D.E., Sahagan, B.G., Morgan, T.E., Finch, C.E., St Laurent, G. 3rd, Kenny, P.J. and Wahlestedt, C. (2008) Expression of a noncoding RNA is elevated in Alzheimer's disease and drives rapid feed-forward regulation of beta-secretase. *Nat. Med.*, **14**, 723–730.
36. Kang, M.J., Abdelmohsen, K., Hutchison, E.R., Mitchell, S.J., Grammatikakis, I., Guo, R., Noh, J.H., Martindale, J.L., Yang, X., Lee, E.K. *et al.* (2014) HuD regulates coding and noncoding RNA to induce APP→Aβ processing. *Cell Rep.*, **7**, 1401–1409.
37. Yoon, J.H., Abdelmohsen, K., Srikantan, S., Yang, X., Martindale, J.L., De, S., Huarte, M., Zhan, M., Becker, K.G. and Gorospe, M. (2012) lincRNA-p21 suppresses target mRNA translation. *Mol. Cell*, **47**, 648–655.
38. Abdelmohsen, K., Panda, A.C., Kang, M.J., Guo, R., Kim, K., Grammatikakis, I., Yoon, J.H., Dudekula, D.B., Noh, J.H., Yang, X. *et al.* (2014) 7SL RNA represses p53 translation by competing with HuR. *Nucleic Acids Res.*, **42**, 10099–10111.
39. Carrieri, C., Cimatti, L., Biagioli, M., Beugnet, A., Zucchelli, S., Fedele, S., Pesce, E., Ferrer, I., Collavin, L., Santoro, C. *et al.* (2012) Long non-coding antisense RNA controls Uchl1 translation through an embedded SINEB2 repeat. *Nature*, **491**, 454–457.
40. Taliaferro, J.M., Lambert, N.J., Sudmant, P.H., Dominguez, D., Merkin, J.J., Alexis, M.S., Bazile, C. and Burge, C.B. (2016) RNA sequence context effects measured in vitro predict in vivo protein binding and regulation. *Mol. Cell*, **64**, 294–306.
41. Dominguez, D., Freese, P., Alexis, M.S., Su, A., Hochman, M., Palden, T., Bazile, C., Lambert, N.J., Van Nostrand, E.L., Pratt, G.A. *et al.* (2018) Sequence, structure, and context preferences of human RNA binding proteins. *Mol. Cell*, **70**, 854–867.
42. Flores, J.K. and Ataide, S.F. (2018) Structural changes of RNA in complex with proteins in the SRP. *Front. Mol. Biosci.*, **5**, 7.
43. Luo, Z., Yang, Q. and Yang, L. (2016) RNA structure switches RBP binding. *Mol. Cell*, **64**, 219–220.
44. Legnini, I., Morlando, M., Mangiacavalli, A., Fatica, A. and Bozzoni, I. (2014) A feedforward regulatory loop between HuR and the long noncoding RNA linc-MD1 controls early phases of myogenesis. *Mol. Cell*, **53**, 506–514.
45. Dimartino, D., Colantoni, A., Ballarino, M., Martone, J., Mariani, D., Danner, J., Bruckmann, A., Meister, G., Morlando, M. and Bozzoni, I. (2018) The long Non-coding RNA linc-31 interacts with Rock1 mRNA and mediates its YB-1-dependent translation. *Cell Rep.*, **23**, 733–740.
46. Li, W., Wang, Q., Feng, Q., Wang, F., Yan, Q., Gao, S.J. and Lu, C. (2019) Oncogenic KSHV-encoded interferon regulatory factor upregulates HMGB2 and CMPK1 expression to promote cell invasion by disrupting a complex lincRNA-OIP5-AS1/miR-218-5p network. *PLoS Pathog.*, **15**, e1007578.
47. Sato, H., Tsukada, T., Nagayoshi, M., Ikawa, Y., Aizawa, S. and Kato, M.S. (1995) Repression of p53-dependent sequence-specific transactivation by MEF2c. *Biochem. Biophys. Res. Commun.*, **214**, 468–474.
48. Zhang, H., Liu, W., Wang, Z., Meng, L., Wang, Y., Yan, H. and Li, L. (2018) MEF2C promotes gefitinib resistance in hepatic cancer cells through regulating MIG6 transcription. *Tumori*, **104**, 221–231.